University of North Carolina Asheville
Journal of Undergraduate Research
Asheville, North Carolina
May 2022

Expression of LuxS and Synthesis of S-Ribosylhomocysteine-Based Covalent Inhibitors of Quorum Sensing in Bacterial Biofilms

Julia McAfee
Department of Chemistry & Biochemistry
The University of North Carolina Asheville
One University Heights
Asheville, North Carolina 28804 USA

Faculty Advisor: Dr. Caitlin McMahon

Abstract

Antibiotic resistance is a growing issue worldwide, therefore there is a pressing need to find a new strategy to fight off bacterial infections. Anti-virulence is a strategy designed to disarm rather than kill bacteria, eliminating the bacteria's evolutionary pressure to become resistant. One virulence factor target is the formation of biofilms. Biofilms are layers of bacteria within a hydrated matrix of polysaccharides and proteins enabling them to defend against antibiotics and the host immune system. Bacteria use quorum sensing to communicate through signaling molecules called autoinducers (AI), triggering gene expression changes which lead to biofilm formation. The AI-2 pathway operates in Gram-positive and Gram-negative bacteria, making it an attractive target for broad spectrum biofilm inhibition. The AI-2 signaling molecule derives from 4,5-dihydroxypentane-2,3-dione (DPD) which results from cleavage of S-ribosyl-L-homocysteine (SRH) by the S-Ribosylhomocysteinase enzyme, LuxS. The main goal of this research is to inhibit LuxS through covalent inhibition. To create a covalent inhibitor for the LuxS protein, molecules will be synthesized to mimic SRH with different electrophiles attached to react with the nucleophilic cysteine in the active site of LuxS. These inhibitors will be synthesized by coupling an electrophilic tail to L- homoserine. To test these inhibitors, LuxS was expressed and purified to be used in later enzyme-based inhibition assays. Computational docking was used to test the binding affinity of proposed inhibitor structures and guide the planning of other new potential inhibitors.

1. Introduction

Antibiotic resistance is a growing problem across the United States. According to the Centers for Disease Control (CDC), there are over 2.8 million antibiotic resistant infections per year, resulting in over 35,000 deaths.[1] Antibiotics are used to treat and prevent bacterial infection by killing bacteria and thus preventing the infection from spreading. However, antibiotic overuse can lead to resistance. Antibiotics are overused in treatment of humans and in livestock. This is problematic because mutated resistant bacteria in animals can be passed down to the consumer or can contaminate the produce from that livestock facility.[2] Once resistance to a certain antibiotic develops in a bacterial strain, it becomes much more challenging to treat that type of infection.

Anti-virulence is a strategy designed to disarm rather than kill bacteria. These types of treatment attack virulence factors rather than eradicating the cells completely, allowing for control of infection without killing the bacteria.[3] Virulence factors are the defense mechanisms used by bacteria, viruses, and fungi to infect and ensure their niche within the host. These virulence factors include quorum sensing, toxin production, and biofilm formation.[4] Targeting virulence factors, instead of using antibiotics, relieves some of the evolutionary pressure selecting for antibiotic resistant bacteria while still allowing for effective treatment of infections.

Anti-virulence strategies are currently being explored through several different approaches, including inhibiting bacterial adhesion to the host cell, inhibiting toxins or specialized secretion systems, and interfacing with gene

regulation of virulence traits.[5] Pilicides have been shown effective as anti-adhesion inhibitors against uropathogenic *E. coli* infections (UPEC). UPEC uses pili to adhere to the host cell, while pilicides mimic the UPEC pilin subunits, preventing the growing formation and adherence of the pili. In an animal study of UPEC infected mice, the pilicides decreased the bacterial adhesion to the bladder preventing the infection in the higher structures of the urogenital tract.[6] The FDA has also approved an anti-virulence treatment for botulism, a rare illness that is caused by neurotoxins secreted from the bacterium *Clostridium botulinum*. A decade-long clinical study with infants have shown immunoglobulins purified from plasma to be effective in inactivating the neurotoxins, resulting in prevention of further intoxication of motor neurons.[7]

Another bacterial virulence factor is biofilm formation. Biofilms are bacteria immobilized into layers of a hydrated matrix of polysaccharides and protein that wraps around a bacterial colony giving it an extra wall of defense. While antibiotics can target and kill free floating bacteria, they will often fail to eradicate the bacteria embedded in biofilm.[8] Bacteria in biofilms are more resistant to antibiotics because the structure of biofilms allows bacteria to remain hidden and become more resistant to treatment. Biofilms resist antibiotics by creating a physical barrier preventing drug penetration, expressing multidrug efflux pumps, and transforming the susceptible planktonic cells into antibiotic resistant persisters, which can lead to chronic infections.[9] Biofilms are formed first through bacterial attachment to a surface (Fig 1), commonly bone or epithelium (digestive and excretory tissue). The second stage is the formation of microcolonies. The third and fourth stages are biofilm maturation and detachment, which can lead to colonization in a new area.[10]

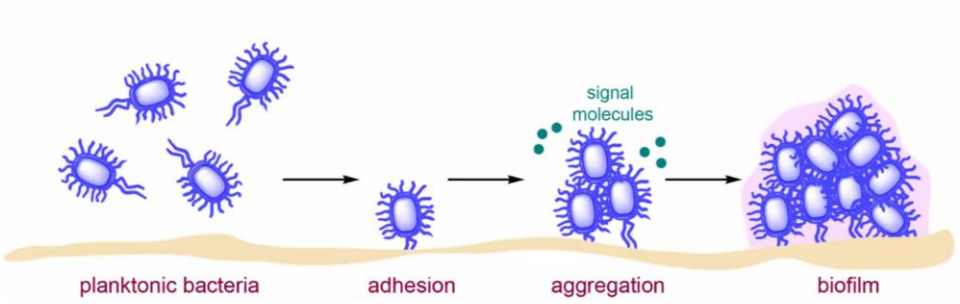

Figure 1. Biofilm formation process (McMahon)

Many processes can be used to inhibit biofilm formation by targeting adhesive organelles, carbohydrates binding adhesins, and quorum sensing. Quorum sensing is a process of cell-to-cell communication in which information is transferred about cell density, resulting in adjustment of gene expression.[11] To do this, bacteria synthesize signaling molecules called autoinducers (AI). When a high enough threshold concentration of autoinducers is met, changes in gene expression are triggered, leading to biofilm formation. Previous research has shown that inhibiting the quorum sensing pathway is an effective method to treat bacterial infections. In a mouse study done by Givskiv et al., researchers used a halogenated furanone to inhibit both Las and Rhl quorum sensing pathway in *P. aeruginosa*, resulting in an average of three orders of magnitude lower bacterial content than the placebo groups.[12]

For this study, the AI-2 pathway (Fig 2) was chosen because it is an inter-species signaling molecule which makes it an interesting and promising broad-spectrum target.[13] In the AI-2 pathway, the molecule S-D-ribosyl-L-homocysteine (SRH) is cleaved by the LuxS enzyme to produce 4,5-dihydroxypentane-2,3-dione (DPD), which is the important precursor to the AI-2 signaling molecule. By preventing LuxS from synthesizing the AI-2 signaling molecule, quorum sensing and thus biofilm formation can be disrupted.[14]

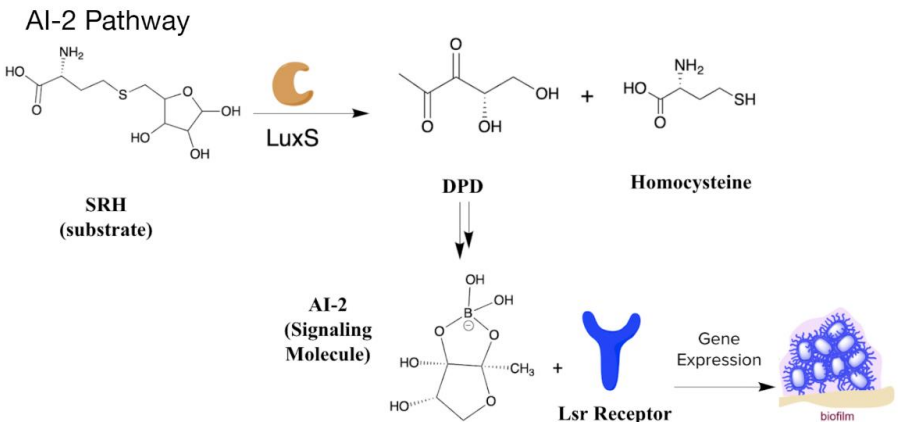

Figure 2. AI-2 Pathway (McMahon)

LuxS inhibitors will be synthesized to optimize covalent inhibition. Covalent inhibition is a two-step process, the first step involves an inhibitor reversibly associating with a target enzyme to bring the chemical warhead of the inhibitor within proximity of the targeted reactive residue in the enzyme. Once in place, a reaction occurs between the inhibitor and the enzyme to form a covalent bond, rendering the enzyme irreversibly inert. However, there are some drawbacks of covalent inhibitors. Covalent drug metabolites have been shown to negatively affect human health. Metabolites of acetaminophen, for example, have been found to be hepatotoxic. There is also a concern for if the inhibitor causes non-specific covalent drug protein interactions, which would lead to unwanted immunogenic responses. Fortunately, not every covalent drug will produce toxic metabolites and undesirable pharmacokinetic properties and covalent drugs are commonly used in a variety of medications including aspirin, acetaminophen, and penicillin. The selectivity of covalent drugs can also be improved to decrease off-target effects. It has been shown that covalent inhibitors have much stronger target binding affinity than reversible inhibitors resulting in prolonging patients' lives. Given the benefits of covalent inhibitors, the development of covalent drugs has been thriving in the past decade.[15]

Covalent inhibitors are attractive targets for LuxS because a nucleophilic cysteine is present in the active site at position 84. LuxS is a Fe^{2+}dependent homodimeric metalloenzyme that is composed of two identical tetrahedral metal-binding sites. The enzyme has a Zn^{2+} metal center coordinated by two histidines, a cysteine, and a solvent molecule.[16] Figure 3a shows the stereo ribbon drawing of LuxS dimer bound to the 2-ketone intermediate.[17] Figure 3b shows a previously researched effective inhibitor from Dehua et al., along with the stereoview of the electron density of the active site of cocrystallized Co(II)- substituted *B. subtilis* LuxS with their most effective inhibitor (Fig 3c).[18] The C3 hydroxyl (O3) is shown to hydrogen bind to the Glu-57 and the C4 hydroxyl (O4) has shown to hydrogen bond to the Ser-6 side chain. This shows how the homocysteine portion of the inhibitor is essential for binding specificity.

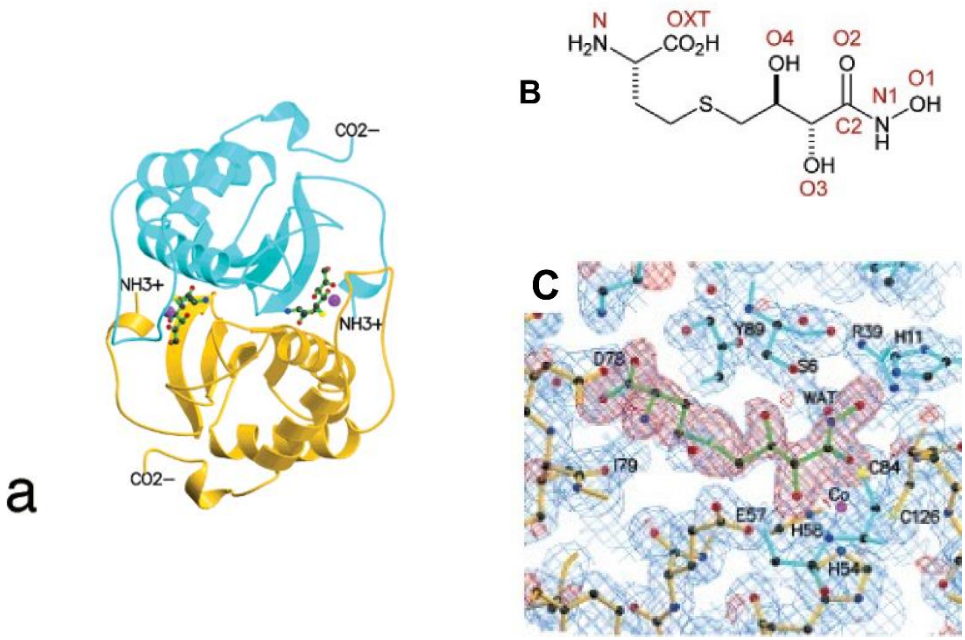

Figure 3. Crystal structure of LuxS in complex with the 2-ketone intermediate: (a) stereo drawing of the LuxS dimer bound to the 2-ketone intermediate. The Co^{2+}ions are shown as purple spheres. (b) designation of atoms and groups in previously researched LuxS inhibitor. (c) stereoview of electron density in the active site with inhibitor. The blue cage is the 1.8 Å $2F_{obsd}$ - F_{calcd} electron density map contoured at 1 σ. 1σ. The red cage is an F_{obsd} -F_{calcd} map, contoured at 2.5σ, calculated before the inhibitor was added to the model. [18]

The goal of this project is to synthesize new drugs to covalently inhibit the enzyme LuxS to disrupt biofilm formation among bacterial infections. The drug would need to covalently bind with the nucleophilic Cys-84 within the active site. Previous research has shown that using an SRH scaffold is effective for specificity, so the homocysteine group will be utilized with an electrophilic tail for covalent binding (Fig 4). The inhibitors will be synthesized utilizing the overall synthetic scheme as shown in Figure 5. Once these inhibitors are synthesized, they will be tested in enzyme-based activity assays to test for the inhibition of LuxS. To run these assays LuxS was transformed, expressed, and purified. A crystal violet staining assay will also be conducted to test specifically for inhibition of biofilm formation along with a *V. harveyi* assay to test for quorum sensing inhibition.

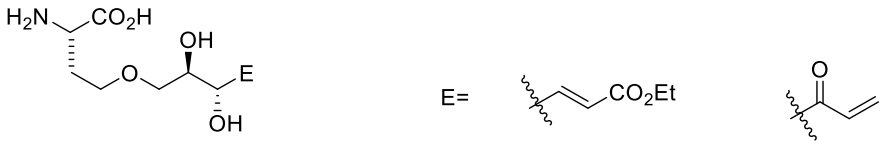

Figure 4. Base inhibitor with homocysteine group and possible electrophiles

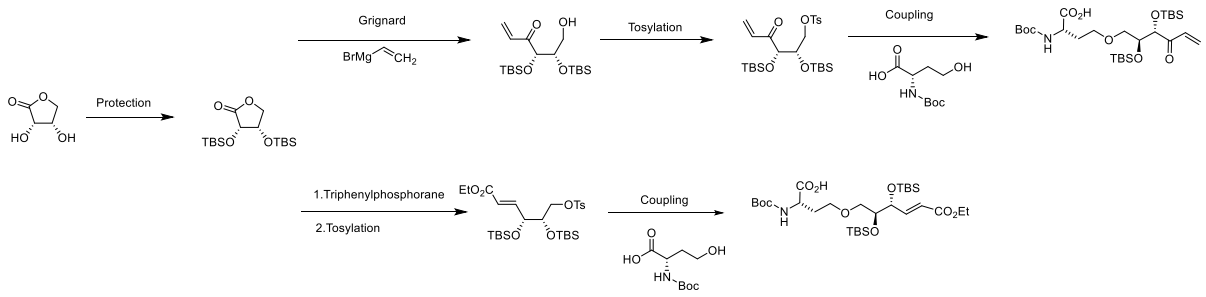

Figure 5. Full synthetic scheme

2. Experimental Methodology

2.1 Biochemical Synthesis General Methods

Biological reagents were purchased from either Alfa Aesar, Acros Organics, or Thermo Fisher Scientific. All sterile equipment was sterilized using an autoclave or passing liquid through a 0.22 μm syringe filter. Biological kits were purchased from New England Biolabs (NEB), and protocols were adapted from given procedures. Samples were centrifuged at 16,000 xg (13,000 RPM) unless stated otherwise. For shaking incubations, samples were incubated in a New Brunswick Excella E25 Incubator Shaker. For non-shaking incubation, a general-purpose incubator for Barnstead Lab-Line was used. For reactions requiring a thermocycler, a BIO-RAD T100 Thermal Cycler was used. DNA was quantified using a NanoDrop microvolume spectrophotometer. LB medium (yeast extract, tryptone, NaCl, and water) was used for liquid cultures and agar plates. For protein expression, minimal media was used, consisting of M9 Salts (3 g/L KH_2PO_4, 12.8 g/L $Na_2HPO_4 \cdot 7H_2O$, .5 g/L NaCl, 1 g/L NH_4Cl), a metal salt mixture (0.5 mM $MgSO_4$, 0.5 μM H_3BO_3, 0.1 μM MnCl2, 0.5 μM $CaCl_2$, 10 μM $CuSO_4$, 1 nM ammonium molybdate), 0.25 % D-glucose, 2 μg/mL thiamin, 1 μg/mL D-biotin, and 0.1 % $(NH_4)_2SO_4$. Medias were supplemented with 50 μg/mL of ampicillin. Gel electrophoresis was run at 90 V using a TAE buffer (0.8 mM tris free base, .04 mM disodium EDTA, and 0.4 mM glacial acetic acid) and a 1% gel consisting of agarose in TAE buffer and 2.5 μL of 10 mg/mL ethidium bromide.

2.1.1 transformation of pET-22b+ to competent DH5α cells

Vector stock (1μL of 100 ng/mL) was gently flicked to mix into the DH5α cells. The tube was set on ice for 30 minutes then heat shocked in a dry bath at 42 °C for 30 seconds. The tube was then placed back on ice for an additional 30 minutes. SOC outgrowth medium (950 μL) was then added. The mixture was placed in a shaking incubator at 37 °C at 250 rpm for 1 hour. Three 10-fold dilutions were then performed by mixing 10 μL of the cell solution placed in a tube with 90 μL of SOC medium and mixed and was repeated twice for the other two dilutions. Each dilution (100 μL), along with the original mixture, was platted on to Luria-Bertani (LB) ampicillin agar plates and incubated at 37 °C overnight to grow. The bacteria were able to grow on the ampicillin plates showing successful transformation.

2.1.2 inoculation of liquid bacterial culture of colony transformed with pET-22b+

Liquid LB (10 mL) was added to sterile 50 mL conical tube along with 10 μL of thawed 100 mg/mL Ampicillin stock resulting in a 50 μg/mL ampicillin concentration. The conical tube was inverted to mix. Media (2 mL) from the conical tube was inserted into 3 culture tubes, two samples and one control. A colony from the 100 X dilution plate was picked off with a pipette tip and dropped into one of the liquid culture tubes. For the control sample, a sterile pipette was dropped into the conical tube. The culture tubes were loosely covered with their caps and placed into a shaking incubator at 250 rpm at 37 °C for about 19 hours. The tubes showed evidence of bacteria growth, so the sample was able to be used to isolate the plasmid.

2.1.3 miniprep plasmid purification

A Monarch Miniprep kit (NEB) was used according to the manufacturer's instructions to isolate the plasmid. The inoculated bacteria (1 mL) were centrifuged, and the supernatant was discarded. The pellet was then resuspended in plasmid resuspension buffer and vortexed to mix until no visible clumps remained. The cells were then lysed with plasmid lysis buffer. The tube was inverted 5-6 times until the color turned dark pink. It was then incubated at room temperature for 1 minute before lysate was then neutralized by plasmid neutralization buffer. The tube was gently inverted until the solution turned uniformly yellow and a precipitate formed. This was then incubated at room for temperature 2 minutes and the lysate was clarified by centrifuging for 5 minutes at 13,000 rpm. To ensure the pellet was compacted it was centrifuged for an additional 2 minutes. The supernatant was then transferred to a spin column and centrifuged for 1 minute at 13,000 rpm. The flow though was discarded.

The column was reinserted in the collection tube and plasmid wash buffer (200 μL) was added to remove RNA, protein, and endotoxins. This was centrifuged for 1 minute at 13,000 rmp and the flow through was discarded. Plasmid wash buffer 2 (400 μL) was added and centrifuged for 1 minute at 13,000 rmp. The column was then transferred into a microfuge tube and autoclaved DI water was added to the center of the matrix and was incubated at room temperature for 1 minute before being centrifuged to elute the DNA. The samples were stored into a -20 °C freezer. Everything

was done twice for the two inoculation samples. The samples were then quantified via Nanodrop. Sample 1 contained 225.1 ng/µL and sample 2 contained 25.3 ng/ µL.

2.1.4 restriction enzyme digest of pET-22b+ plasmid

Purified pET-22b+ plasmid vector DNA (4.44 µL) was transferred into microcentrifuge tubes. 10x CutSmart buffer (5 µL) was pipetted into the tube then sterile DI water (38.6 µL) was added. XhoI enzyme (1 µL) and NdeI enzyme (1 µL) was added to the tube and were incubated overnight at 37 °C. This was repeated for both purified samples. A gel electrophoresis was run to test to see if the restriction enzymes had successfully cut the plasmid. A 1% agarose gel was made for electrophoresis. Digested DNA samples were mixed with loading dye (1 µL) before DNA (5 µL) was placed into the well. The original plasmid (2 µL) was mixed with deionized water (3 µL) and loading dye (1 µL) as a control. NEB quick load ladder (5 µL) was inserted into lane 1, original pET-22b+ plasmid (6 µL) into lane 2, and 6 µL of each digested sample was put into lane 3 and lane 4. The gel was run at 90 V for 1 hour and 30 minutes.

2.1.5 clean up of digested pET-22b+ plasmid samples

Ethanol (20 mL) was added to the DNA wash buffer. DNA clean up binding buffer (90 µL) was added to the digested plasmid to dilute it. It was then centrifuged in a spin column for 1 minute at 13,000 rmp. The flow through was discarded and DNA wash buffer (200 mL) was added. It was then centrifuged for another minute at 13,000 rmp. This was repeated two times before transferring the column to a 1.5 centrifuge tube with DI water (200 mL). It was then incubated for one minute at room temperature, then was put back in the centrifuge for 1 minute at 13,000 rmp. It was then quantified to be 149.4 ng/µL and 97.4 ng/µL.

2.1.6 ligation Assembly of LuxS- pET-22b+

To make a 100 ng/µL stock, 12.79 µL of nuclease free water was added to 1279 µL/mL of the LuxS DNA stock. It was then diluted to 10 ng/µL by 1 µL of the 100 ng/µL stock being added to 9 µL of deionized water. On ice NEB Hifi DNA assembly master mix (5 µL) was put into a PCR tube with nuclease free water (2.784 µL), linearized pET-22b+ (1 µL), and 10 ng/µL LuxS DNA (1.216 µL). For a no insert control Hifi DNA assembly master mix (5 µL) was added with linearized pET-22b+ (1 µL) and deionized water (4 µL) into a PCR tube. A positive control was prepared by adding Hifi DNA assembly master mix (5 µL) and NEB positive control (5 µL). All tubes were incubated in a thermocycler at 50°C for 15 minutes. Each reaction (2 µL) was then mixed with DH5α cells and a transformation procedure was performed as described above.

2.1.7 sequencing preparation

Stocks of promoter and terminator primers (10 µM) were prepared. Nucleus free water (167.3 µL) was added to 10 ng of T7 promoter primer and nuclease free water (171.4 µL) was added to T7 terminator primer (10 µL). Both samples were then centrifuged for 30 seconds at 13,000 rpm. In a PCR strip tube 80.2 ng/µL purified DNA (11 µL) was added with 10 µM promoter primer (1 µL). The second sample was made by adding 11 µL of 80.2 ng/µL purified DNA to 1 µL of 1 µM terminator primer. Both samples were stored in the -20 °C freezer.

2.1.8 isolation and purification of LuxS-pET22b+ plasmid

A liquid culture was performed using a colony from the 1:10 diluted colony 1 plate and the 1:100 colony 2 plate. Two colony were also taken from the PCR colony 1 plate and two colony from the PCR colony 3 plate. The samples were miniprepped and purified and quantified to be 149.6 ng/µL, 328.6 ng/µL, 163 ng/µL, and 368.2 ng/µL. The samples with higher concentrations allowed for further sequencing and transformations. 10 samples were sent out to Genomic Sciences Laboratory at NC state university be sequenced and matched the expected sequence with the LuxS insert.

2.1.9 transformation of LuxS-pET22b+ to BL21 DE3 cells

A tube of BL21 DE3 E. coli cells were thawed on ice for 10 minutes. DNA (1 µL) from the 1:100 colony 2 miniprep was mixed in with the cells. The mixture was incubated on ice for 30 minutes then heat shocked at 42 °C for exactly

10 seconds. The cells were then placed on ice for 5 minutes before room temperature SOC (950 µL) was added. The mixture was then incubated at 37 °C shaking at 250 rpm for 1 hour. The cells were diluted 10-fold three times with the SOC medium. Each cell mixture (100 µL) was spread on ampicillin plates and incubated at 37 °C overnight. This was done a second time with PCR colony 3 miniprepped DNA (2.72 µL) that was diluted with water (7.28 µL) since the sequencing came back confirmed for that plasmid.

2.1.10 protein expression of LuxS

A liquid culture was created with minimal media (10 mL) and a colony from the new BL21 DE3 cell transformation. The culture was incubated with shaking at 120 rpm at 37 °C overnight. The culture (10 mL) was then diluted into minimal media (990 mL) and incubated at 37 °C while shaking at 120 rmp. Every hour for three hours the OD600 was measured, although due to inconsistencies the culture was left to grow for a full day at 37 °C with shaking. Afterwards the OD600 was measured to be 0.614, so induction was performed by adding $CoCl_2$ stock (846 µL) and IPTG stock (1 mL). The cells were left to incubate for 5 hours at 30 °C. The measured sample (25 µL) was taken and spun in the centrifuge at 3000 gx for 5 minutes then the supernatant was discarded and stored in the -20 °C freezer for 5 hours. The OD600 was then measured again reading 0.5700, so 23.21 µL of the sample was spun down at 3000 xg for 3 minutes and stored in the freezer. A big culture was then spun in the centrifuge at 4000 xg at 4 °C for 20 minutes. The supernatant was then discarded, and the remaining sample as stored in a conical tube at -20 °C.

2.2 Computational Docking Methods

Programs used were ChemDraw 19.0, Chem3D 19.0, AutoDockTools and Autodock Vina 1.5.7, PyMol, and Rosetta Software Suite.

2.2.1 preparing protein for AutodockTools (ADT)

The protein used for LuxS was the crystal structure of 2FQO. The file was downloaded from Protein Data Bank website as a .pdb file. The .pdb file was opened in ADT to delete the water and add hydrogens. The protein was then saved as a .pdbqt file to be used in docking.

2.2.2 preparing inhibitors for AutodockTools

The proposed inhibitors were designed in ChemDraw and saved as .cdx files. The .cdx file was visualized in Chem3D and saved as a Protein Data Bank format (.pdb). In ADT the .pdb file was opened as Ligand. Under Torsion Tree the root was detected. The ligand was outputted as a .pdbqt file. The prepared protein .pdbqt file was opened. A grid box was placed over the targeted Cys-84 binding site on the protein. A configuration .txt file was saved using the protein .pdbqt file as the receptor and the .pdbqt file of the inhibitor as the ligand. The config.txt file was run in Autodock Vina using vina.exe to run the docking program. The top 9 binding affinities were calculated in kcal/mol and visualized using the output .pdqt file in PyMol.

2.2.3 submitting inhibitors into Rosetta Server

All proposed inhibitors were drawn in chemdraw and saved as a .cdx file. The cdx files were saved as .pdb files via Chem3D. The pdb files were opened in Pymol to add hydrogens before saving them as a .SDF file for upload. All inhibitors were uploaded as [Ligand_docking]. The parameters were left as default setting except for “generate ligand conformers with BCL” and “use the starting coordinates in SDF”. Protein 2fqo was uploaded from the Protein Data Bank website.

2.3 Chemical Synthesis General Methods

Chemicals were purchased from Alfa Aesar, Acros Organic, and Thermo Fisher Scientific. Reactions were concentrated under reduced pressure via Heidolph rotary evaporator unless otherwise noted. Thin Layer

chromatography (TLC) was performed on SilliaPlates from Silicycle and were visualized with either UV or potassium permanganate stain ($KMnO_4$) unless otherwise noted. Flash column chromatography was performed using silica gel (SiO2, 40-63 µm, 230-400 mesh). Proton nuclear magnetic resonance spectra (^1H NMR) were recorded on a 400 MHz Varian NMR spectrometer with solvent resonance as the internal standard (^1H NMR: $CDCl_3$ at 7.27 ppm) unless otherwise stated. ^1H NMR data are reported as follows: chemical shift, multiplicity (s = singlet, d = doublet, t = triplet, q = quartet, dd = doublet of doublets, ddd = doublet of doublet of doublets, m = multiple, br = broad) and integration.

2.3.1 protection of D-erythronolactone[19]

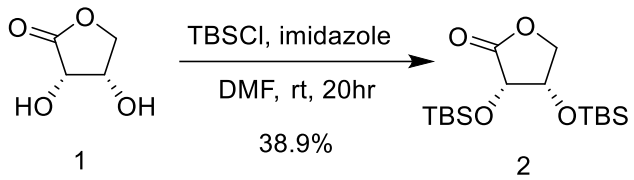

A solution was made by dissolving lactone (**1**) (1 equiv, 17.61 mmol, 2.0800 g) in a solution of dry dimethylformamide (DMF) (88.06 mL, 0.2 M) then was cooled in an ice bath (0 °C). After the solution cooled, imidazole (6 equiv, 105.68 mmol, 7.1942 g) was added. In one portion, TBSCl (6 equiv, 105.68 mmol, 15.9276 g) was added and the solution was stirred at room temperature overnight. The reaction was then quenched with saturated aqueous NH_4Cl and diluted with diethyl ether. After the layers were separated, the aqueous layer was extracted with two portions of ether. The organic layers were combined and then washed with H_2O and brine then dried over anhydrous $MgSO_4$. The solution was then filtered and concentrated. Half of the crude product (~5g) was purified by column chromatography (10:1 hexanes:ethyl acetate) and was monitored by TLC and visualized with $KMnO_4$. The desired produced resulted in a white solid (1.187 g, 38.9 %). ^1H NMR ($CDCl_3$, 400 MHz): δ 4.4 (dd, 1H), 4.3 (d, J = 10 Hz, 1H), 4.25 (dd, 1H), 4.2 (d, 1H), 0.9 (s, 9H), 0.8 (s, 9H), 0.3 (d, 6H), 0.2 (d, 6H).

2.3.2 tosylation of compound 4[20]

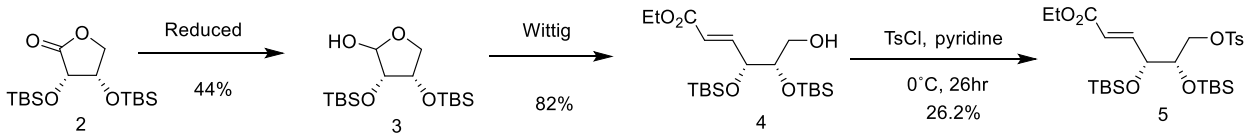

Under an argon balloon, the previously made alcohol (**4**) (1 equiv, 0.4776 mmol, 160 mg) was stirred with pyridine (1.0 mL, 0.46 M) in an ice bath (0 °C). Toluenesulfonyl chloride (2 equiv, 0.9553, 182 mg) was then added to the stirred solution and the mixture was stirred for about 24 hours. The reaction was monitored through TLC (1:1 ethyl acetate: hexane). Pyridine was co-evaporated with 3 portions of toluene (2 mL) and concentrated. The crude product was taken up in ethyl acetate and was washed with 2 portions of $NaHCO_3$ and 1 portion of brine. The organic layer was separated out and dried over $MgSO_4$. The product was concentrated as a white solid and an NMR was taken in $CDCl_3$. To purify, column was run in 10:1 Hexane: ethyl acetate and was monitored by TLC and visualized with UV and $KMnO_4$. The first spot off the column yielded the desired product of an oil (0.253 g, 26.2 %). ^1H NMR ($CDCl_3$, 400 MHz): δ 7.80 (d, 2H), 7.2 (d, 2H) 6.99 (dd, 1H), 5.99 (dd, 1H), 4.25 (dd, 1H), 4.17 (q, 2H), 4.07 (q, 1H), 3.78 (ddd, 1H), 3,5-3.6 (m, 2H), 2.5 (s, 3H), 1.99 (dd, 1H), 1.3 (dd, 3H), 1.0 (m, 18H), 0.08-0 (m, 12H).

2.3.3 coupling reaction of previously made protected L-homocysteine with compound 5[21]

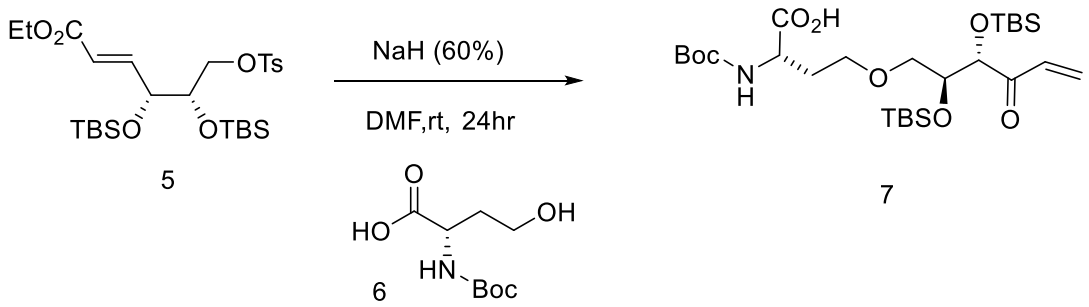

A stirred solution of purchased homoserine (**6**) (1 equiv, 0.1 mmol, 0.0219 g) was dissolved in DMF (0.3 mL, 0.33 M). The solution was then cooled in an ice bath (0 °C) before NaH (60%) (2.5 equiv, 0.01 g) was slowly added. After gas evolution ceased, compound (**5**) (1 equiv, 0.1 mmol, 0.0573g) was added and stirred at room temperature for 24 hours. The solution was then cooled in an ice bath (0 °C) before being diluted with ethyl acetate (30 mL) and H_2O (50 mL). The organic layer was separated and washed with H_2O and brine twice. The solution was then dried over Na_2SO_4 filtered and concentrated. An NMR sample was prepared in deuterated chloroform. The NMR spectrum showed mostly starting material and a contamination between peaks 7-8. The reaction was not successful.

2.3.4 grignard reaction of protected D-erythronolactone with vinyl magnesium bromide [22]

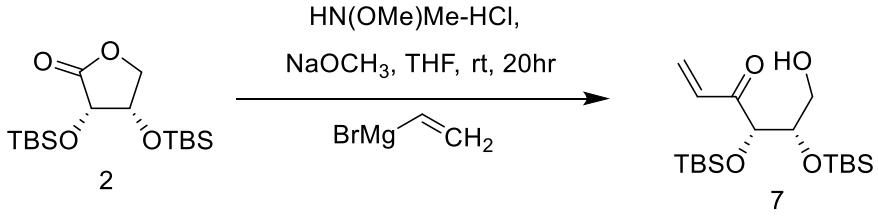

The protected lactone (2) (1 equiv, 1.44 mmol, 0.500 g) was dissolved in anhydrous THF (28.86 mL, 0.05 M). Then HN(OMe)Me-HCl (1.2 equiv, 1.7306 mmol, 0.1688 g) and $NaOCH_3$ (0.25 equiv, 0.3606 mmol, 0.0195 g) was added, and the solution was cooled on an ice salt bath (-15 °C). The vinyl magnesium bromide (8 equiv, 11.540 mmol, 16.4857 mL) was then very slowly added, and the reaction was run at room temperature overnight. The reaction was then quenched with 1N HCl solution (10 mL) then was continued to stir for 2 hours. The THF was then evaporated. The sample was then treated with H_2O and extracted with DCM and dried over $MgSO_4$. The crude product resulted in a orange oil. The product was purified by column chromatography in a 3:4 hexane: ethyl acetate mobile phase. It was monitored by TLC and visualized through UV. Some of spot 1 was able to be isolated, but all of spot two came out mixed with spot 1. An NMR sample was prepared with deuterated chloroform of spot 1. The NMR showed that the product was not purified.

3. Results and Discussion

The transformation of pET-22b+ to competent DH5α cells and its amplification in liquid bacterial culture were successful. After miniprep isolation, the samples were quantified, and a decent yield of plasmid was obtained. The sample was then digested using XhoI and NdeI restriction enzymes. To test if the digestion worked, gel electrophoresis was done with the digested DNA, the stock plasmid, and the mini-prepped DNA. After cleaning up the samples, they were quantified via Nanodrop measuring concentrations of 149.4 ng/µL and 97.4 ng/µL. The gel showed the restriction enzymes had successfully cut the plasmid (Fig 6). It showed evidence that the plasmid was successfully cut by only showing 1 band in lane 3 representing the linearized digested plasmid, unlike in lane 2 and 4 that show 2 circular conformations of the plasmid.

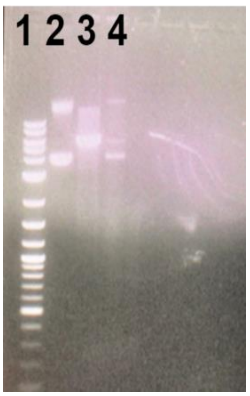

Figure 6. Gel electrophoresis to assess digestion
Lane 1: ladder, Lane 2: original pET-22b+ plasmid, Lane3: digested plasmid sample 1, Lane 4: minipreped plasmid

During the ligation step, 3 reactions were performed. The first sample was LuxS pET-22b+ DNA and for the control linearized pET-22b+ was ligated. For a positive control, the ligation was done with the NEB positive control. All samples were then transformed to DH5α cells and were spread onto agar ampicillin plates. The bacteria with a no insert control did not grow on the ampicillin agar plate which suggests that that the original cut out piece from the plasmid was successfully removed, since it did not reform. Our positive control did grow on the ampicillin plate which showed that the condition and reagents worked. The sample with the LuxS DNA did grow which suggests that our ligation step worked, and the plasmid is circular. The resulting DNA samples were extracted and sent out to be sequenced to confirm LuxS was inserted. A gel was also run to ensure ligation was successful (Fig 7).

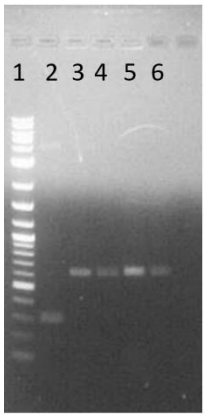

Figure 7. Gel run for ligation test with PCR products. Lane1: ladder, Lane 2: LuxS- pET-22b+ plasmid, Lane 3: colony 1, Lane 4: colony 2, Lane 5: colony 3, Lane 6: colony 4.

The gel was run with 4 PCR products from different colonies from the ligation plates. Lane 2 showed the pET-22b+ plasmid PCR product as a control. Lanes 3-6 were the PCR products from the ligation plates. The gel showed the ligation PCR products to weigh the accurate amount of the LuxS gene suggesting the ligation was successful. A PCR product was also sent out to a sequencing lab ensuring the ligation was successful.

When LuxS was ready for biological and inhibition assays, synthesis of LuxS inhibitors commenced. To synthesize the proposed inhibitors, D-erythronolactone must first be protected before opening the ring with either a Grignard or Wittig reaction. After the Wittig reaction, a Tosylation reaction was done to add a leaving group for coupling with L-homoserine. The protection of the of D-erythronolactone was successful and confirmed via NMR, although only half of the crude product was purified. It had a low percent yield of 38.9%. The protected lactone **2** underwent two different reaction paths. One was prepared by another student in the lab who had reduced the protected lactone, then conducted a Wittig reaction with the reduced protected lactone and triphenylphosphorane yielding compound **4**. This compound then underwent a Tosylation reaction to prepare it for coupling with a protected L-homoserine **6,** that was also prepared

by another student in the lab. The Tosylation reaction successfully yielded an oil product as confirmed by NMR, but with a low yield of 26.2 %. The NMR indicated the product was not 100% pure (there were extra peaks at 0.1 and 0.9 ppm), but it was decided for the product to still undergo the coupling reaction. The coupling reaction with L-homoserine was unsuccessful. According to the NMR, it appears that the majority of the product was unreacted starting material. This reaction will be redone later once more of the Tosylated Wittig product is made.

A second inhibitor was then attempted from the same protected lactone **2**. Rather than reducing the lactone, a vinyl group was added by a Grignard reaction. The NMR spectrum of the crude product looked promising, but the product was unable to be successfully purified by column chromatography. This was probably due to the column being too small and too much DCM being added to dissolve the product, not allowing the desired product to stick to the silica. The purification needs to be redone to isolate the desired compound **7**.

Once compound **7** is purified it will undergo a Tosylation reaction to prepare it for coupling with the protected L-homoserine **6**. Ideally, once the coupling reaction is successful with compound **7** and compound **5**, they will both undergo a deprotection reaction to remove all the protecting groups as seen in Figure 12.

To better understand the LuxS binding pocket and to test the inhibitor's predicted binding affinity, computational docking was done utilizing Autodock Vina. A series of proposed SRH-based inhibitors and structural derivatives were tested with various electrophiles to compare potential binding affinities (Fig 8). Cysteine residues are highly reactive making them an optimal target for covalent inhibition. The top binding position in the correct orientation for each structure is shown in Figure 8.

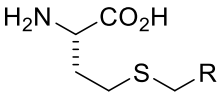

#	Structure	Binding Affinity (kcal/mol)	Distances from Cystine (Å)	Estimated Kd (µM)
1	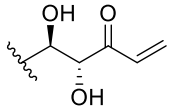	-6.2	3.5	27.03
2	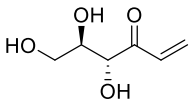	-4.9	4.1	254.74
3	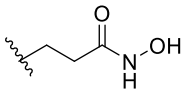	-5.9	4.2	47.06
4	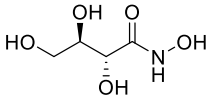	-5.9	4.2	47.06
5	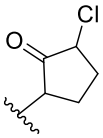	-5.6	3.7	78.11
6	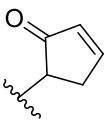	-6.1	4.6	33.57
7		-5.5	3.0	92.48
8	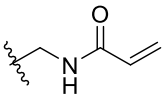	-5.7	4.2	65.97
9	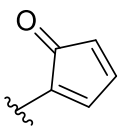	-5.7	3.6	65.97
10	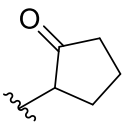	-5.7	4.6	65.97

Figure 8. proposed inhibitors and their binding affinity calculated by ADT

It is important to note that some of the proposed inhibitors that were not in the correct conformation had stronger affinities due to possible closer interactions, although covalent bonding from the electrophilic head of the inhibitor with the nucleophilic Cys-84 would provide a much stronger bond then the binding affinity would account for.

As a control the ligand that was co-crystallized in the 2FQO structure was run in ADT for a comparison (Fig 3b). It resulted in a binding affinity of -6.5 kcal/mol and showed possible hydrogen binding with the oxygen next to the amine with Arg-39 with distances of 3.1 Å and 3.4 Å. There also might be hydrogen bonding occurring between that same oxygen with the oxygen on Ser-6 giving a distance of 3.7 Å. The hydroxyl closest to the sulfur also showed possible hydrogen interactions with Ser-6 also with a distance of 3.7 Å. The ligand was relatively close to the targeted amino acid Cys-84 with a distance of 3.6 Å. The same ligand was also run through Rosetta server due to the server's predictions being more accurate by allowing the protein to be flexible, rather than stationary. Rosetta calculated a binding affinity of -20.47 REU (Rosetta energy units) which is the software's arbitrary units used to make its docking predictions. Rosetta predicted very similar results to ADT (Fig 9), but showed closer interactions between the ligand and the Arg-39 residue with distances of 2.8 Å. It also showed additional interactions with Tyr-89 with a distance of 4 Å but did not show the same interactions with Ser-6 as ADT predicted. In addition, it predicted a slightly further distance from the targeted residue Cys-84 of 3.9 Å. Due to Rosetta's accurate predictions, all proposed inhibitors were also run in Rosetta, but due to technical error it did not dock the inhibitor on the protein, so those predictions were not obtained.

ADT	Binding affinity kcal/mol	Rosetta server	Binding affinity (Rosetta Energy Units)
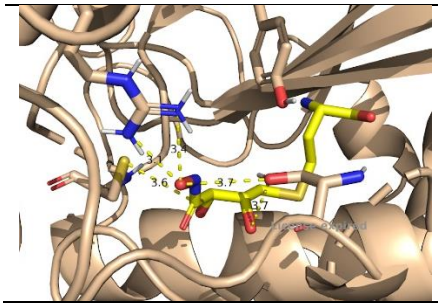	-6.5	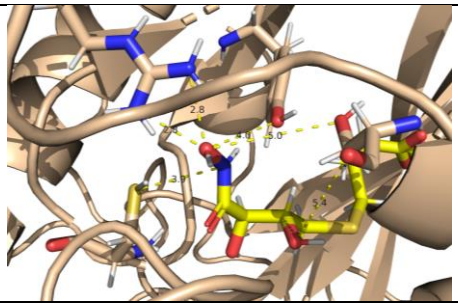	-20.47

Figure 9. Docking images of predicted binding using ADT and Rosetta server of the crystalized ligand visualized in PyMol and their calculated distances from Cys-84 and hydrogen bonding distances

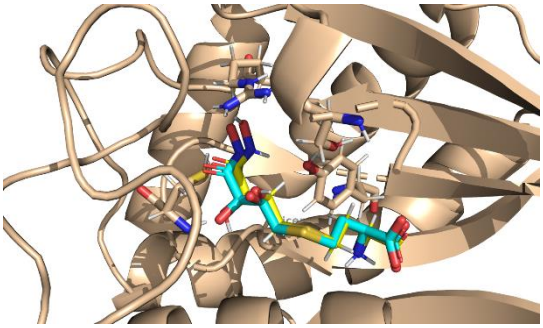

Figure 10. ADT and Rosetta predicted conformation in PyMol. ADT is turquoise and Rosetta is yellow

Almost all the proposed inhibitors were built off the skeleton structure of SRH with varying R groups (Fig 11). Inhibitor 1 had the closest interaction with Cys-84 of 3.5 Å and the highest binding affinity of -6.2 kcal/mol. This is probably because it most closely mimicked SRH out of all the inhibitors allowing it to be highly selective. It showed possible hydrogen binding with Arg-39, Ser-6, and Tyr-89. Inhibitor 2 was the least like SRH and was predicted to

have the weakest binding affinity of -4.9 kcal/mol and a distance of 4.1 Å from Cys-84. It also was in a backwards conformation for its strongest two binding affinity predictions. The only possible hydrogen bonding it showed was with Ser-6 with a distance of 3.2 Å. Inhibitors 3 and 4 were both predicted to have a binding affinity of -5.9 kcal/mol and a distance from the Cys-84 of 4.2 Å. The additional hydroxyl groups on inhibitor 4 showed to provide close hydrogen interactions with Ser-6 and Try-89 that was not seen with inhibitor 3. This suggested the hydroxyl groups provide lots of close hydrogen binding within the active site despite not having the SRH backbone structure.

Inhibitor 6 had the second highest binding affinity of -6.1 kcal/mol despite that it had the largest distance of 4.6 Å from Cys-84. The oxygen coming of the cyclopentane showed possible hydrogen binding with Ser-6, Arg-39, and Tyr-89. Although, none of these interactions were seen in inhibitor 5. Inhibitor 5 had a much weaker binding affinity of -5.6 kcal/mol. This suggests the alkene within the ring may be important for structural support and rigidity of the inhibitor. It is also possible that the Cl may have prevented close interactions from occurring. Inhibitor 10 had the same structure as inhibitor 5, but without the Cl. It is predicted to have a slightly better affinity of -5.7 kcal/mol and showed possible hydrogen binding with Arg-39, Ser-6, and Tyr-89 as seen with inhibitor 6, much a much weaker binding affinity. Inhibitors 9 was tested if 2 alkenes in the ring would improve binding affinities. Similarly, to inhibitor 10 it had a binding affinity of -5.7 kcal/mol, but was unable to hydrogen bond with the oxygen on the cyclopentane. It appears that having two alkenes in the ring may have caused the ring to become too rigid, not allowing it to bend into the best conformation. Inhibitor 7 showed the closest distance from the Cys-84 with a distance of 3.0 Å despite its weaker binding affinity of -5.5 kcal/mol. There only seemed to be possible hydrogen binding with the carboxylic acid with the Tyr-89 residue showing a distance of 3.6 Å. Inhibitor 7 lacks specificity to the binding pocket, but its small electrophilic head provides insight on a closer interaction with Cys-84. The addition of the trans hydroxyl groups may have proved that additional needed specificity while still retaining the close interaction with the Cys-84. Inhibitor 8 had a similar structure to inhibitor 3 with a switched position of the amine and an alkene instead of a hydroxyl. It resulted in a weaker binding affinity of -5.7 kcal/ mol despite having similar hydrogen binding interactions with Arg-39, Ser-6, and Tyr-89. Having the hydroxyl on the end of the inhibitor rather than the alkene seems to provide better closer hydrogen interactions.

#	Docking imaging	#	Docking imaging
1	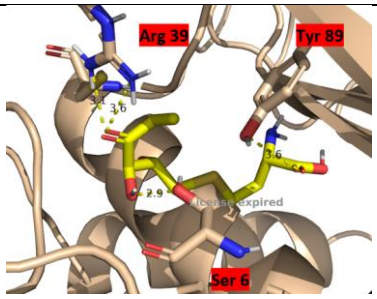	**6**	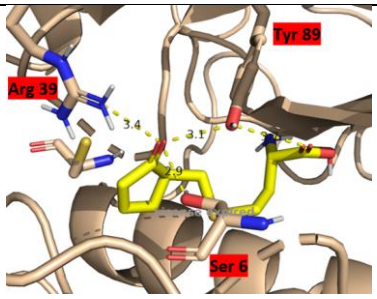
2	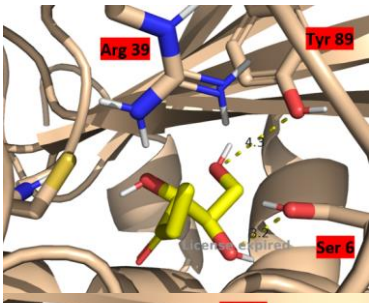	**7**	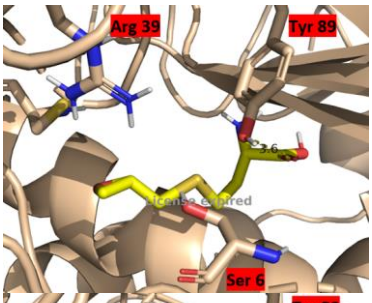
3	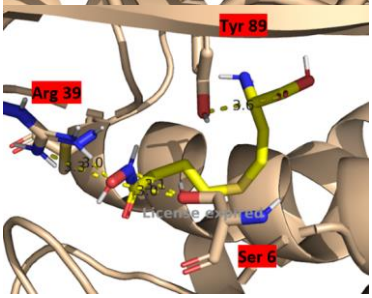	**8**	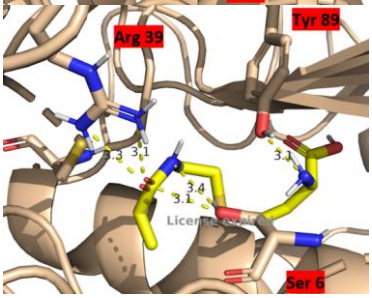
4	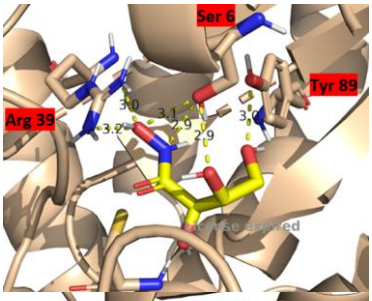	**9**	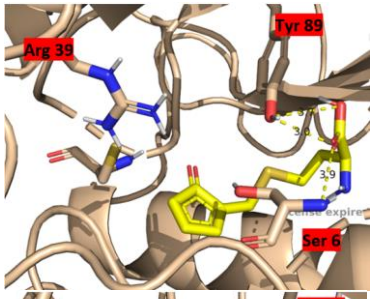
5	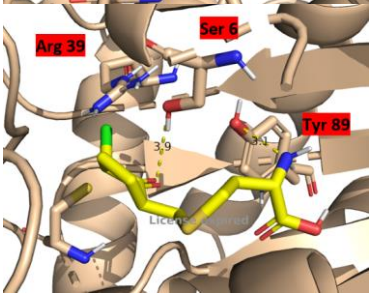	**10**	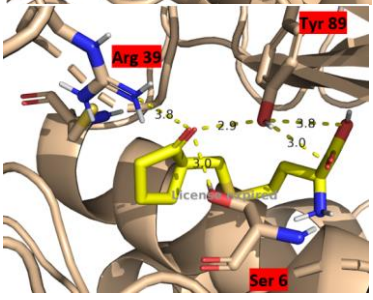

Figure 11. Docking images of proposed inhibitors visualized in PyMol and their possible hydrogen bonding with Ser-6, Arg-39, Tyr-89

The binding affinity determined by ADT Vina was used to determine an estimate of the inhibitors' K_d which represents the concentration of the inhibitor needed for 50% binding.

$$K_d = e^{\Delta G/RT} \quad (1)$$

Equation (1) was used to determine the concentration (μM) of the inhibitor needed. R represented the gas constant 1.987 cal·K^{-1}·mol^{-1} and T for temperature 298 K. The binding affinity was inserted for ΔG as cal/mol. Based on these calculations, the inhibitor with the weakest binding affinity would have a K_d of 254.74 μM whereas the inhibitor with the strongest binding affinity would have a K_d of 27.03 μM, approximately a 10-fold difference. By analyzing this docking data a proposed synthetic scheme has been made (Fig 12).

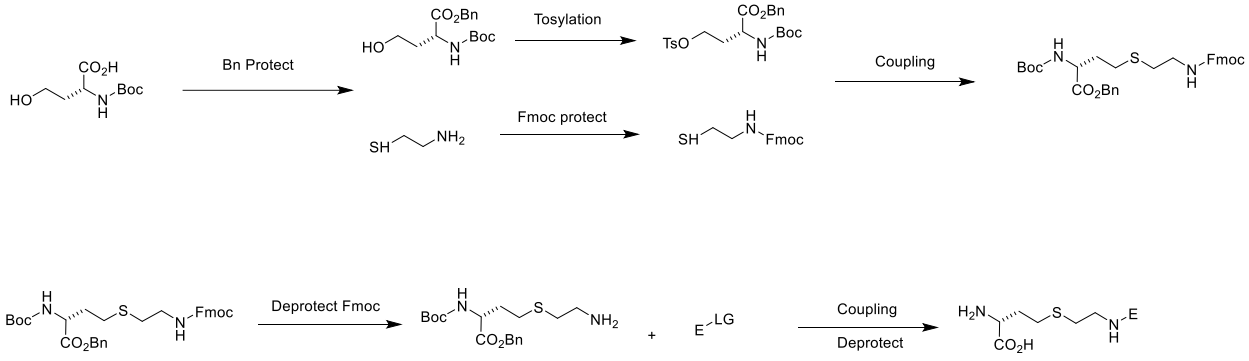

Figure 12 New synthetic scheme for future inhibitors

The scheme starts with a protection of the carbonyl on L-homoserine as a benzyl ester. The hydroxyl group would then be converted to a leaving group such as a mesylate or tosylate. Meanwhile, the cysteamine needs to undergo an amine protection with Fmoc to be coupled with L-homoserine product. After coupling the products, the Fmoc protecting group would need to be deprotected to allow the amine from the cysteamine to react with different possible electrophiles with a leaving group. Once coupled the amine and the carbonyl from the L- homoserine would be deprotected resulting in any final inhibitors. Additionally, when the scheme shown in Figure 5 is completed, a deprotection step would be conducted to get to the final inhibitor (Fig 13).

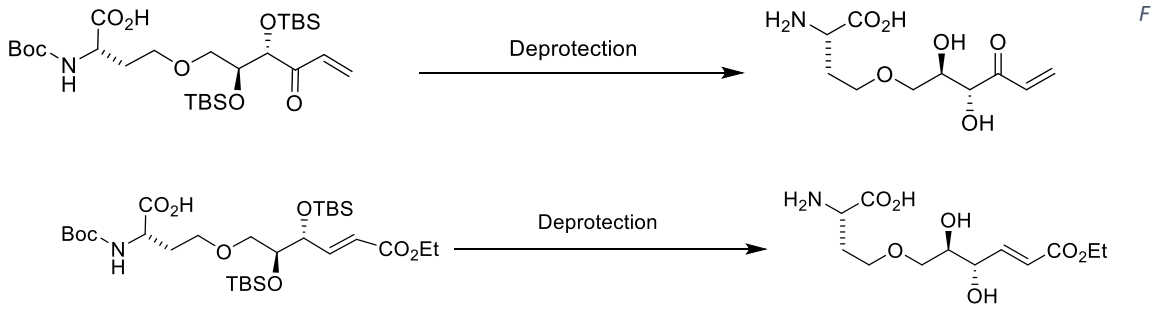

Figure 13. Deprotection of coupled products from compounds 5 and 7 resulting in final inhibitor

Once the inhibitor and the natural substrate for LuxS, SRH are synthesized, enzyme-based activity assays can be conducted to test for inhibition of LuxS. The biofilm inhibition can also be tested by conducting a crystal violet staining assay. To test is the quorum sensing is specifically being inhibited, a quorum sensing assay will be conducted with *V. harveyi*. Additional docking may be conducted to gain better insight on new possible inhibitors.

4. Conclusion

LuxS was able to be successfully isolated and expressed and was purified over the summer by another student. LuxS is now ready to be used in future inhibition assays. Two inhibitor types are in the process of being synthesized. Once the coupling reaction with compounds **5** and **7** with the protected L-homocysteine **6** is completed, they will be deprotected and ready for testing. For future inhibitor ideas, other electrophiles will be added to other SRH based inhibitors. Docking was conducted to investigate other possible residues that can be targeted within the binding pocket of LuxS. This information provided important information of how the structure of inhibitors will affect binding affinity within the binding pocket. A new synthetic scheme was proposed for future synthesis of new possible covalent inhibitors. This information may provide new insight on anti-virulence approaches, biofilm inhibition, and the inhibition of LuxS. The proposed LuxS inhibitors may also provide a possible new outlook towards fighting bacterial biofilms through irreversible covalent inhibition.

5. Acknowledgements

Special thank you to Dr. Caitlin McMahon for the opportunity and guidance through this research project, and to my lab partner Jake Wilkinson for all their help, the UNC Asheville Department of Chemistry and Biochemistry for providing the resources and lab to conduct this research.

6. References

1. Biggest Threats and Data. https://www.cdc.gov/drugresistance/biggest-threats.html (accessed Oct 21, 2020).
2. Antibiotic Resistance, Food, and Food Animals. https://www.cdc.gov/foodsafety/challenges/antibiotic-resistance.html (accessed Nov 18, 2020).
3. Totsika, M. Benefits and Challenges of Antivirulence Antimicrobials at the Dawn of the Post-Antibiotic Era. *Drug Delivery Letters* **2016**, 6 (1), 30–37.
4. Sharma, A. K., Dhasmana, N., Dubey, N., Kumar, N., Gangwal, A., Gupta, M., & Singh,Y. Bacterial Virulence Factors: Secreted for Survival. *Indian journal of microbiology* **2017**, 57 (1), 1–10.
5. Rasko, D., Sperandio, V. Anti-virulence strategies to combat bacteria-mediated disease. *Nature Reviews Drug Discovery 9* **2010**, 117–128.
6. Svensson A, Larsson A, Emtenäs H, Hedenström M, Fex T, Hultgren SJ, Pinkner JS, Almqvist F, Kihlberg J. Design and evaluation of pilicides: potential novel antibacterial agents directed against uropathogenic Escherichia coli. *Chembiochem*. **2001**; 2(12):915-8.
7. Dickey, Seth W.; Cheung, Gordon Y. C.; Otto, Michael. Different drugs for bad bugs: antivirulence strategies in the age of antibiotic resistance. *Nature Reviews Drug Discovery* **2017**, (16), 457–471.
8. Philip S Stewart, J William. Costerton. Antibiotic resistance of bacteria in biofilms. *The Lancet* **2001**, 358 (9276), 135-138.
9. Leid, J. G. Bacterial Biofilms Resist Key Host Defenses. *Microbe* **2009**, 4 (2), 66–70.
10. Crouzet, M., Le Senechal, C., Brözel, V. S., Costaglioli, P., Barthe, C., Bonneu, M., Garbay, B., & Vilain, S. Exploring early steps in biofilm formation: set-up of an experimental system for molecular studies. *BMC microbiology* **2014**, 14, 253.
11. Rutherford ST, Bassler BL. Bacterial quorum sensing: its role in virulence and possibilities for its control. *Cold Spring Harb Perspect Med* **2012**, 2(11) :a012427.
12. Hentzer, M., Wu, H., Andersen, J. B., Riedel, K., , T. B., Bagge, N., Kumar, N., Schembri, M. A., Song, Z., Kristoffersen, P., Manefield, M., Costerton, J. W., Molin, S., Eberl, L., Steinberg, P., Kjelleberg, S., Høiby,

N., & Givskov, M. Attenuation of Pseudomonas aeruginosa virulence by quorum sensing inhibitors. *The EMBO journal* **2003**, 22(15), 3803–3815.
13. Quan, Y., Meng, F., Ma, X. et al. Regulation of bacteria population behaviors by AI-2 "consumer cells" and "supplier cells". *BMC Microbiol* **2017**, 198 (17).
14. Xu L, Li H, Vuong C, Vadyvaloo V, Wang J, Yao Y, Otto M, Gao Q. Role of the luxS quorum-sensing system in biofilm formation and virulence of Staphylococcus epidermidis. *Infect Immune* **2006**, 74(1), 488-96.
15. A. K. Ghosh, I. Samanta, A. Mondal, W. R. Liu. *ChemMedChem* **2019**, 14, 889.
16. Hilgers, M. T.; Ludwig, M. L. Crystal structure of the quorum-sensing protein LuxS reveals a catalytic metal site. *Proceedings of the National Academy of Sciences* **2001**, 98(20), 11169–11174.
17. Rakhi Rajan, Jinge Zhu, Xubo Hu, Dehua Pei, and Charles E. Bell., Crystal Structure of S-Ribosylhomocysteinase (LuxS) in Complex with a Catalytic 2-Ketone Intermediate. *Biochemistry* **2005**, 44 (10), 3745-3753
18. Gang Shen, Rakhi Rajan, Jinge Zhu, Charles E. Bell, and Dehua Pei,. Design and Synthesis of Substrate and Intermediate Analogue Inhibitors of S-Ribosylhomocysteinase. *Journal of Medicinal Chemistry* **2006** 49 (10), 3003-3011
19. Pramod K. Sahu, Gyudong Kim, Jinha Yu, Ji Yoon Ahn, Jayoung Song, Yoojin Choi, Xing Jin, Jin-Hee Kim, Sang Kook Lee, Sunghyouk Park, and Lak Shin Jeong. Stereoselective Synthesis of 4′-Selenonucleosides via Seleno-Michael Reaction as Potent Antiviral Agents. *Organic Letters* **2014**, 16 (21), 5796-5799
20. M.E. Bolitho et al./ Revisiting synthetic preparation of the quorum sensing substrate S-d-ribosyl-l-homocysteine (SRH). *Carbohydrate research* **2014**, 394, 32-38.
21. Daqiang Li, Xiaotuan Zhang, Xiaodong Ma, Lei Xu, Jianjun Yu, Lixin Gao, Xiaobei Hu, Jiankang Zhang, Xiaowu Dong, Jia Li, Tao Liu, Yubo Zhou, and Yongzhou Hu. Development of Macrocyclic Peptides Containing Epoxyketone with Oral Availability as Proteasome Inhibitors. *Journal of Medicinal Chemistry* **2018,** 61 (20), 9177-9204
22. Shao-Bo Yang, Feng-Feng Gan, Guo-Ju Chen, Peng-Fei Xu. An Efficient One-Pot Synthesis of ω-Hydroxy Ketones from Lactones. *Synlett* **2008,** (16): 2532-2534